Solid-State Chemistry

Pillared Hybrid Solids with Access to Coordinatively Unsaturated Metal Sites: An Alternative Strategy**

Paul A. Maggard, Bangbo Yan, and Junhua Luo*

Porous solids that contain accessible, coordinatively unsaturated (open) metal sites within a rigid framework show great potential for applications in catalysis, absorption of gases (H_2 and CH_4), and small-molecule recognition,[1–4] as highlighted in recent reviews.[5,6] There is a growing interest to improve catalytic and gas-absorption selectivity through the immobilization of reactive transition-metal centers inside highly functionalized, size-selective pores. This is envisioned as an extension of the well-known catalysis mediated by zeolite solids and coordination compounds. However, only a few mixed examples of open-framework solids with access to open metal sites have been reported, including open Zn, Cu, and Tb sites in three distinct metal–organic frameworks,[3,4,7] and Ni and Co sites within separate metal–hydroxycarboxylate solids.[8,9] These open metal coordination sites are typically obtained post-synthesis upon removal of a terminal ligand (such as H_2O or pyridine) from the metal without irreversible destabilization or collapse of the pore structure. The carboxylate functional groups of the ligands convey much of the structural stability in the above examples.

[*] Prof. P. A. Maggard, Dr. B. Yan, Dr. J. Luo
Department of Chemistry, North Carolina State University
Raleigh, NC 27695 (USA)
Fax: (+1) 919-515-5079
E-mail: paul_maggard@ncsu.edu

[**] The authors acknowledge the assistance of C. Day and J. Folmer. This work was supported by the ACS Petroleum Research Fund (#40963-G10) and the NCSU Faculty Research and Professional Development Fund.

By contrast, our research efforts are directed toward the use of metal oxide/organic assemblies, in which a robust metal oxide layer serves as the general platform to both immobilize and help structurally stabilize the open metal sites. The general approach is shown in Scheme 1, and arose from the

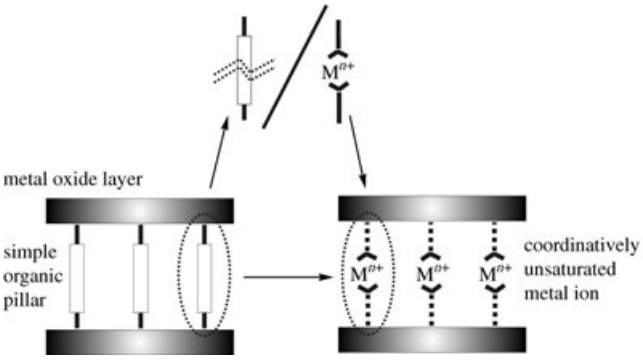

Scheme 1. The general strategy of substituting a symmetrical bridging ligand with an unsymmetrical ligand that results in access to open metal sites between metal oxide layers.

discovery and subsequent structural analysis of $Cu_2(pzc)_2(H_2O)_2ReO_4$ (pzc = 2-pyrazinecarboxylate),[10] which consists of $CuReO_4$ layers separated by pillars of $[Cu(pzc)_2(H_2O)_2]$. The strategy is based on substitution of the simple bridging ligand of a pillared solid for one that exhibits two different bonding preferences: one that favors attachment to the metal oxide layer and the other, to the desired transition metal. The ligand-bonding preferences can be used to entrain specific transition metals between the metal oxide layers. Furthermore, if the functional groups of the ligand satisfy the charge requirements of the transition metal (for example, two carboxylates for one M^{II}), then other neutral terminal ligands can be removed post-synthesis to yield open metal sites. The potential application of this synthetic strategy to immobilize open metal sites is also relevant to the large numbers of pillared layered phosphonates, sulfates, and hydroxide structures such as those reported earlier.[11–15] Herein we report the first description and application of this novel general strategy to target open Co and Ni sites stabilized between $AgReO_4$ layers.

The starting point of our synthesis was the simple, recently synthesized[16] $AgReO_4(pyz)$ (pyz = pyrazine) pillared solid shown in Figure 1a, which contains neutral $AgReO_4$ layers pillared by pyrazine. As suggested in Scheme 1, this synthesis was modified by using 2-pyrazinecarboxylate in place of pyrazine and adding Co^{II} and Ni^{II} for inclusion between the layers. Standard hydrothermal techniques were used and the reactants were heated at $\approx$110–140 °C for 24 h, followed by slow cooling for 24 h. Orange $Co(pzc)_2(H_2O)_2AgReO_4$ (**1**) and irregular platelike green crystals of $Ni(pzc)_2(H_2O)_2AgReO_4$ (**2**) were obtained and characterized by X-ray diffraction.[17] The reversible removal of coordinated H_2O was detected by thermogravimetric analysis (TGA).

The structures of both solids (Figures 1b and c) derive from that of $AgReO_4(pyz)$ in which $AgReO_4$ layers are bridged through pzc to interlayer Co or Ni centers in **1** and **2**,

 DOI: 10.1002/ange.200462715

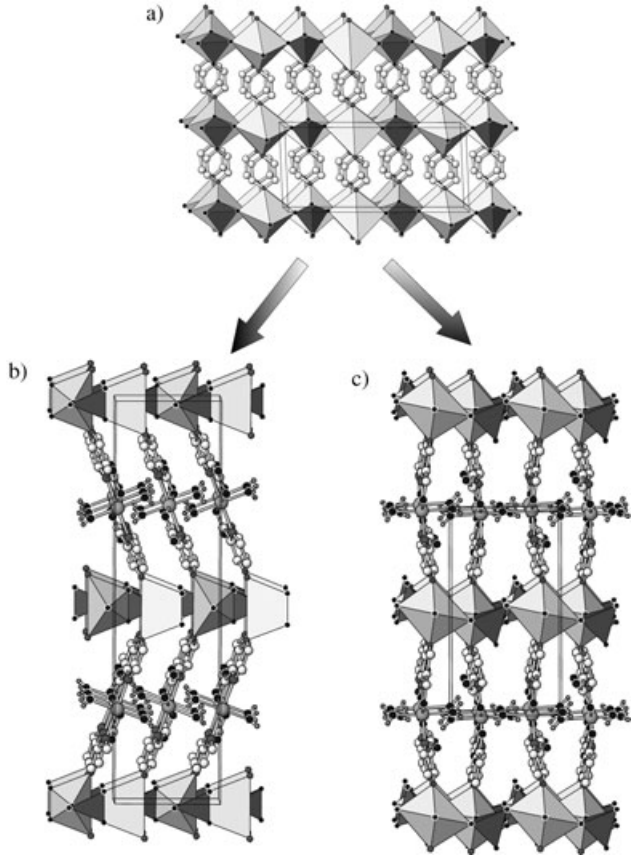

Figure 1. Layered structure views of a) $AgReO_4(pyz)$; b) $Co(pzc)_2(H_2O)_2AgReO_4$; and c) $Ni(pzc)_2(H_2O)_2AgReO_4$. $AgReO_4$ layers are illustrated with polyhedra; light polyhedra are Ag-centered, dark represent ReO_4^-; interlayer atoms: black = O, darkly shaded = N, white = C, and lightly shaded = Co and Ni.

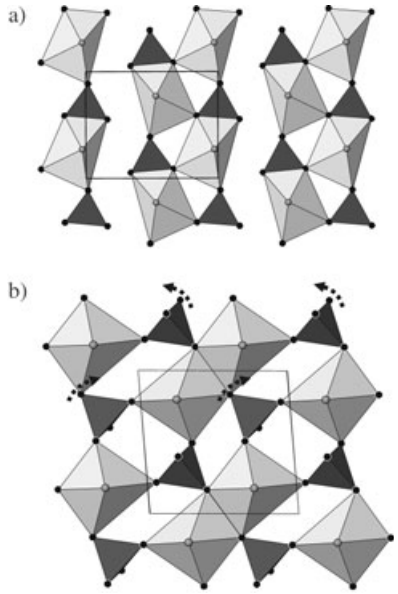

Figure 2. Polyhedral view normal to the $AgReO_4$ layers for a) **1** and b) **2**; dashed arrows denote rotations to interrelate the orientations of ReO_4^- tetrahedra between the two structures.

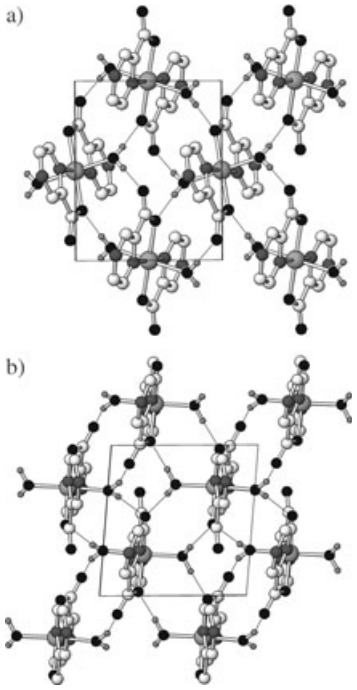

Figure 3. View of a single layer of $M(pzc)_2(H_2O)_2$ pillars drawn normal to the layer plane with the unit cell outlined: a) M = Co and b) M = Ni; interlayer atoms: black = O, darkly shaded = N, white = C, lightly shaded = Co and Ni, and gray = H.

respectively. The $[Co(pzc)_2]$ pillars in **1** are tilted with respect to the $AgReO_4$ layers, resulting in a relatively smaller interlayer spacing of $\approx$13.58 Å (*b*-axis/2), whereas the $[Ni(pzc)_2]$ pillars in **2** buckle only slightly with a *c*-axis layer spacing of $\approx$14.00 Å. The lone (*para*) N atoms of the pzc ligands bond preferentially to the Ag sites of the $AgReO_4$ layer with Ag–N bond lengths of 2.214(3) Å in **1** and 2.246(6) and 2.258(6) Å in **2**. Within the $AgReO_4$ layers of both structures, the ReO_4^- tetrahedra have regular Re–O bond lengths in the range of 1.680(6)–1.765(7) Å (Figure 2). The 2D packing of the $AgReO_4$ layers is structurally similar in **1** and **2**, with the ReO_4^- tetrahedra in approximately body-centered arrangements with Ag-centered polyhedra on the edges. However, in **2** there are two distinct sets of tetrahedral orientations that alternate, which causes the changes in local Ag atom environments. A rotation of each ReO_4^- tetrahedron in **2** by $\approx$20–25° that aligns them in a single direction brings this layer into closer similarity to the topology of **1** (Figure 2b).

The COO^- groups and N atoms of the pzc ligand preferentially coordinate to the equatorial positions of Co and Ni at the usual distances (2.026(5)–2.169(2) Å)[18,19] as shown in Figure 3. The COO^- groups and N atoms on opposing ligands arrange *trans* with respect to each other. The axial positions of the metals are bonded by H_2O, at distances of 2.060(2) Å for Co and 2.033(6) and 2.086(6) Å for Ni. In both **1** and **2**, each H_2O molecule forms H bonds (Figure 3, thin lines: OH···O) at distances of 1.75–2.13 Å to both O atoms of the carboxylate groups. However in **2**, an O atom of one carboxylate group has no H-bond contacts whereas the other has two. This difference results from the tilt of the $[Co(pzc)_2]$ pillars, in

contrast to the nearly vertical pillars of $[Ni(pzc)_2]$. The metal-bridged pillars are bonded to the $AgReO_4$ layers, which structurally separate and hinder the Co/Ni sites from further bonding to free carboxylate groups as frequently occurs in metal–organic structures.[19,20] This feature also helps prevent structural collapse upon removal of coordinated H_2O from the Co/Ni centers.

TGA performed under flowing N_2 showed a mass loss that corresponds to the removal of coordinated H_2O (calcd, 5.1%; exptl, 5.2%) at 120°C for **1** and 170°C for **2**. TGA curves for both are shown as insets in Figure 4. Concomitant color changes were observed as lighter shades of orange and green for **1** and **2**, respectively. Further decomposition occurred at >300°C; the compounds exhibited a total range of stability close to 200°C. Both could be rehydrated with drops of H_2O on a glass slide, and subsequent TGA again revealed the characteristic 5% mass loss for all coordinated H_2O, an indication for porosity.[21] Full rehydration required only minutes for **1**, but up to 20 h for **2**. This is likely the result of the much larger crystal sizes of **2** (>×50, on average) and longer H_2O diffusion paths than present in **1**.

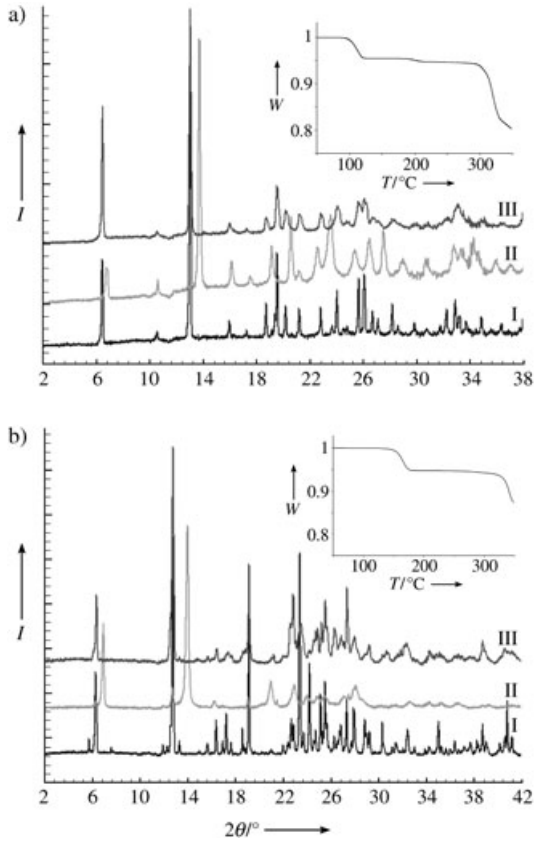

Figure 4. Powder X-ray diffraction results for a) **1**, and b) **2**; directly post-synthesis (I), after dehydration (II), and after rehydration (III); insets: respective TGA curves (w = mass fraction).

Powder X-ray diffractometry was used to monitor the rate and effect of rehydration and dehydration on both structures (Figure 4). After one cycle of dehydration/rehydration, **1** and **2** showed almost no change in peak position, and slightly less crystallinity. Shifts in peak position were noticeable upon dehydration, corresponding to decreases in the $AgReO_4$ interlayer spacing (≈0.73 Å for the (020) and (040) planes for **1;** ≈1.34 Å for the (001) and (002) planes for **2**). The larger decrease in interlayer spacing for **2** is likely caused by the nearly vertical orientation of the $[Ni(pzc)_2]$ pillars in the hydrated state, which results in a more dramatic tilt (and compression) upon the removal of H_2O. Both dehydrated structures stabilize at a similar interlayer spacing of ≈12.8–13.0 Å.

The substitution of pyrazine for 2-pyrazinecarboxylate pillars between $AgReO_4$ layers, as diagrammed in Scheme 1, results in solids **1** and **2** that are predisposed to the formation of coordinatively unsaturated Ni and Co sites. Ongoing investigations of the Cu analogue show structural similarity, but a dehydrated and novel chiral framework that results from significant tilting of the pillars.[22] A recent synthesis of sulfate analogues suggest that strong coordination preferences of the organic pillars will be essential for the success of this strategy.[23] Notably, other examples of hybrid solids that use 2-pyrazinecarboxylate but contain tubelike structures have been reported; such hybrids exhibit porosity.[19] However, very few synthetic approaches are known that enable access to a similar diversity of open late-transition-metal sites within closely related hybrid solids.

Experimental Section

1: Product was obtained by hydrothermal reaction (1 g total) of Ag_2O (0.313 mmol), Re_2O_7 (0.313 mmol), 2-pyrazinecarboxylate (1.251 mmol), $Co(OH)_2$ (0.625 mmol), and distilled H_2O (31.26 mmol). All chemicals were used as received with stated purities of >99%. Reactants were loaded and sealed inside a teflon pouch, which was placed inside a teflon-lined stainless-steel reaction vessel (120 mL). The vessel was heated to and kept at 125°C for 36 h, and gradually cooled to room temperature over 24 h. The products consisted of large orange crystals and powder in typical yields of >90% based on Co.

2: Product was obtained by hydrothermal reaction of starting materials listed above for **1** in similar molar ratios and NiO (0.633 mmol) in place of $Co(OH)_2$. The reactants were heated at 140°C for 36 h, and gradually cooled to room temperature over 24 h. The products consisted of green crystals in >90% yield based on Ni.

Received: November 24, 2004
Published online: March 16, 2005

Keywords: cobalt · hydrothermal synthesis · microporous materials · nickel · solid-state structures

[1] N. Guillou, Q. Gao, P. M. Forster, J.-S. Chang, M. Nogues, S.-E. Park, G. Férey, A. K. Cheetham, *Angew. Chem.* **2001**, *113*, 2913; *Angew. Chem. Int. Ed.* **2001**, *40*, 2831.
[2] P. M. Forster, J. Eckert, J.-S. Chang, S.-E. Park, G. Férey, A. K. Cheetham, *J. Am. Chem. Soc.* **2003**, *125*, 1309.
[3] H. Li, C. E. Davis, T. L. Groy, D. G. Kelley, O. M. Yaghi, *J. Am. Chem. Soc.* **1998**, *120*, 2186.
[4] B. Chen, M. Eddaoudi, T. M. Reineke, J. W. Kampf, M. O'Keefe, O. M. Yaghi, *J. Am. Chem. Soc.* **2000**, *122*, 11559.
[5] P. M. Forster, A. K. Cheetham, *Top. Catal.* **2003**, *24*, 79.
[6] M. J. Rosseinsky, *Microporous Mesoporous Mater.* **2004**, *73*, 15.

[7] T. M. Reineke, M. Eddaoudi, M. Fehr, D. Kelley, O. M. Yaghi, *J. Am. Chem. Soc.* **1999**, *121*, 1651.
[8] P. M. Forster, A. K. Cheetham, *Angew. Chem.* **2002**, *114*, 475; *Angew. Chem. Int. Ed.* **2002**, *41*, 457.
[9] S. O. H. Gutschke, D. J. Price, A. K. Powell, P. T. Wood, *Eur. J. Inorg. Chem.* **2001**, 2739.
[10] J. Luo, B. Alexander, T. R. Wagner, P. A. Maggard, *Inorg. Chem.* **2004**, *43*, 5537.
[11] A. Clearfield, *Chem. Mater.* **1998**, *10*, 2801.
[12] A. Clearfield, Z. Wang, *J. Chem. Soc. Dalton Trans.* **2002**, 2937.
[13] G. Alberti, R. Vivani, F. Marmottini, *J. Porous Mater.* **1998**, *5*, 205.
[14] a) A. Rujiwatra, C. J. Kepert, M. J. Rosseinsky, *Chem. Commun.* **1999**, 2307; b) A. Rujiwatra, G. J. Mander, C. J. Kepert, M. J. Rosseinsky, *Cryst. Growth Des.* **2005**, *5*, 183.
[15] K. Susumu, K. Ryo, *Comments Inorg. Chem.* **2002**, *23*, 101.
[16] P. A. Maggard, P. D. Boyle, unpublished results.
[17] Single-crystal data were collected on a Bruker Apex CCD area detector diffractometer with $Mo_{K\alpha}$ radiation ($\lambda = 0.71073$ Å). The data were solved and refined by using SHELXS97 and SHELXL97 within WINGX version 1.64.05.[24] Crystal data for **1**: orange ($0.066 \times 0.080 \times 0.110$ mm^3); $M_r = 699.22$; orthorhombic *Pnma* (no. 62); $a = 7.1029(6)$, $b = 27.160(2)$, $c = 8.7482(8)$ Å, $V = 1687.7(2)$ Å^3; $Z = 4$; $T = 293(2)$ K; $\rho_{calcd} = 2.752$ g cm^{-3}; $\mu = 9.337$. Crystal data for **2**: green ($0.18 \times 0.18 \times 0.03$ mm^3); $M_r = 699.00$; triclinic $P\bar{1}$ (no. 2); $a = 7.5795(9)$, $b = 7.8800(9)$, $c = 14.0052(9)$ Å, $\alpha = 83.271(2)$, $\beta = 89.660(3)$, $\gamma = 85.156(3)°$, $V = 827.75(15)$ Å^3; $Z = 2$; $T = 193(2)$ K; $\rho_{calcd} = 2.805$ g cm^{-3}; $\mu = 9.654$. For **1** and **2**, Final R/R_w on $|F^2|$ were 0.027/0.064 (2591 data) and 0.058/0.167 (5188 data) with GOF = 1.09 and 1.07, and max/min residual electron densities of 2.21/−0.7 and 4.75/−4.48. CCDC-257420 (**1**) and -257421 (**2**) contain the supplementary crystallographic data for this paper. These data can be obtained free of charge from The Cambridge Crystallographic Data Centre via www.ccdc.cam.ac.uk/data_request/cif.
[18] L.-M. Zheng, X. Wang, Y. Wang, A. J. Jacobson, *J. Mater. Chem.* **2001**, *11*, 1100.
[19] L.-M. Zheng, T. Whitfield, X. Wang, A. J. Jacobson, *Angew. Chem.* **2000**, *112*, 4702; *Angew. Chem. Int. Ed.* **2000**, *39*, 4528.
[20] S. K. Dey, B. Bag, K. M. Abdul Malik, M. S. El Fallah, J. Ribas, S. Mitra, *Inorg. Chem.* **2003**, *42*, 4029.
[21] Note: In general, uptake of structural water could also be the result of a dissolution/reprecipitation mechanism in which only subnanomolar concentrations in solution are required. However, powder X-ray diffraction patterns suggest a gradual structural change between the dehydrated and hydrated forms, in contrast to the dissolution mechanism.
[22] Unit cell: $P4_32_12$, $a = 7.612$, $c = 49.4945$ Å.
[23] P. A. Maggard, unpublished results.
[24] L. J. Farrugia, *J. Appl. Crystallogr.* **1999**, *32*, 837.

